DOI: 10.1002/cphc.201200014

Design Rules for Nanogap-Based Hydrogen Gas Sensors

Junmin Lee,[a] Wooyoung Shim,[b] Jin-Seo Noh,*[a] and Wooyoung Lee*[a]

Nanoscale gaps, which enable many research applications in fields such as chemical sensors, single-electron transistors, and molecular switching devices, have been extensively investigated over the past decade and have witnessed the evolution of related technologies. Importantly, nanoscale gaps employed in hydrogen-gas (H_2) sensors have been used to reversibly detect H_2 in an On–Off manner, and function as platforms for enhancing sensing performance. Herein, we review recent advances in nanogap design for H_2 sensors and deal with various strategies to create these gaps, including fracture generation by H_2 exposure, deposition onto prestructured patterns, island formation on a surface, artificial manipulation methods, methods using hybrid materials, and recent approaches using elastomeric substrates. Furthermore, this review discusses a new nanogap design that advances sensing capabilities in order to meet the diverse needs of academia and industry.

1. Introduction

Since the On–Off mechanism of palladium (Pd) was first demonstrated using nanogap-based Pd mesowires, from which originated a new paradigm for detecting hydrogen gas (H_2),[1] significant progress has been made in efforts to realize better-designed nanogap-based H_2 sensors. Unlike other applications using nanosized gaps such as chemical and biosensors,[2–4] single-electron transistors,[5–7] and molecular switching devices,[8–10] where nanogaps play an ancillary role in determining performance, nanogaps in Pd-based H_2 sensors function as a key player for the detection of H_2.[1,11–42] Thus, nanogap design, which allows sensors to exhibit improved performance such as high sensitivity, rapid response, short recovery time, and good reliability, has become a crucial part of H_2 sensing. As a result, techniques for making nanogaps have attracted much interest. A recent study of H_2-induced swelling of cracked Pd thin films represents significant advances in nanogap-based H_2 sensors,[43] in terms of enhancing sensing capabilities, compared to previous approaches, simply by using an elastomeric substrate[44]. Very few studies have addressed design rules for nanogap-based H_2 sensors.[45] Other reviews associated with H_2 sensors have mainly focused on the diversity and dimensionality of sensing materials[46–48] and detection principles.[49–51] For this reason, the aim of hydrogen sensor researchers and manufacturers is to make robust, efficient, and cost-effective nanogap-based devices in a simple manner.

Herein, we highlight the progress to date for nanogap-based H_2 sensors and advanced design rules for H_2 sensors, which have been achieved over the span of the last decade. Methods for creating gaps are classified into multiple categories: fracture generation by H_2 exposure, deposition onto prestructured patterns, island formation on surfaces, artificial manipulation methods, methods using hybrid materials, and the use of elastomeric substrates. This review not only discusses many of the methods currently used for creating gaps for use in H_2 sensors, but also proposes a strategy for a novel design for future H_2 sensors.

2. Two mechanisms at Play

As the need for alternative energy sources has increased,[52] hydrogen gas has received a great deal of attention due to its cleanliness, abundance, and recyclability.[53–55] Consequently, accurate and rapid detection of H_2 is an indispensible prerequisite for its extensive use in various fields, because it is highly flammable and has explosive properties when its concentration exceeds 4% in air.[56] For this reason, diverse approaches have been proposed and implemented to realize optimum H_2 sensors.[57–65] Among them, Pd-based sensors have been widely explored because of the unique ability of Pd to readily dissociate H_2 into H atoms on its surface and then absorb those atoms spontaneously at room temperature.[66] Owing to this property, Pd/H systems have been employed in many hydrogen-related research fields such as hydrogen storage,[67–69] hydrogenation of matter,[70,71] and H_2 sensors.[72–75]

The H_2-sensing mechanisms of Pd-based sensors are classified into two categories. In the first case, H atoms are incorporated into the countinuous Pd structures (without nanogaps) and act as electron scattering sources, so that electrical resistance increases (Figure 1 a).[66] In this case, the electrical resistance increases with the increase in H_2 concentration, because the frequency of electron-H scattering increases as the amount of H atoms in the Pd structures increases. For pure bulk Pd or thin films, it is not likely to provide precise H_2 detection above a certain H_2 concentration where the transition from the α to β phase occurs.[66] In addition, absorption of a large amount of H atoms leads to a significant volume expansion of Pd and re-

[a] J. Lee, Dr. J.-S. Noh, Prof. W. Lee
Department of Materials Science and Engineering
Yonsei University
262 Seongsanno Seodaemun-gu, Seoul, 120-749 (Korea)
Fax: (+82) 2-312-5375
E-mail: wooyoung@yonsei.ac.kr
jinseonoh@yonsei.ac.kr

[b] W. Shim
Department of Materials Science and Engineering
Northwestern University
2145 Sheridan Road, Evanston, IL 60208-3113 (USA)

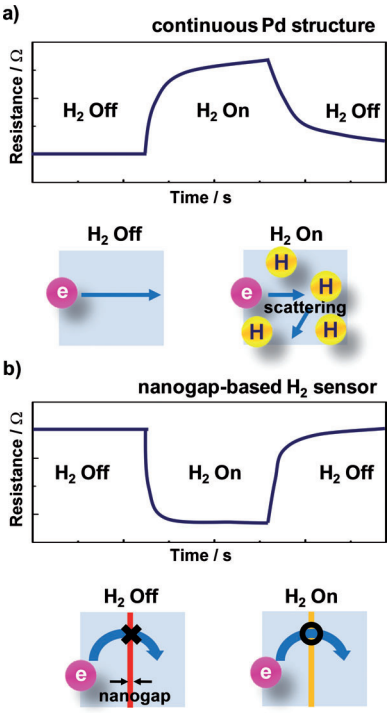

Figure 1. Two mechanisms in play. Representative electrical responses of a) a continuous Pd structure and b) a nanogap-based H_2 sensor. The schematic illustrations below (a) and (b) represent the mechanisms of an increase in the resistance by electron scattering and a decrease in the resistance by nanogap open–close mecahnism, respectively.

sults in structural deformation of Pd bodies, and as a consequence, hysteresis behavior of electrical resistance.[76] These drawbacks can be solved by using Pd alloys with other elements such as Mg,[77] Au,[78] Ag,[79] and Ni.[80] However, this approach is associated with disadvantages such as a slow response time, long recovery time, low sensitivity, and a shifted base resistance. Nevertheless, due to easy fabrication and a low detection limit, many studies have been conducted using continuous Pd structures.

The second category is based on the nanogap structure.[1,11–42] When a Pd structure is exposed to H_2, a Pd/H solid solution is formed at low H_2 concentrations. At high concentrations of H_2, there is a 3.5% volume expansion due to the numerous H atoms incorporated into Pd.[1] Importantly, this is the basis of many studies that have utilized nanogaps for Pd-based H_2 sensors. Since nanogaps in Pd structures interfere with electric current flow, volume expansion after H_2 exposure allows the nanogaps to be closed, leading to a substantial inflow of electrical current. As a result of employing the nanogap designs, the electrical resistance (conduction) of H_2 sensors abruptly decreases (increases) when exposed to H_2 and recovers to the initial base resistance (base conduction is zero) after removal of H_2 (Figure 1b). This means that sensors with complete nanogaps can function as On–Off switches. Nanogap-based sensors exhibit many benefits such as a short response time, a large On-Off ratio in electrical signals, and improved reliability. However, they are unable to detect low concentrations of H_2. This is because the mechanism is based on the event triggered by volume expansion of Pd that occurs mainly during the phase transition of Pd at H_2 concentrations ranging from 1 to 2% at room temperature.[66] As such, a huge number of studies have been conducted in an attempt to overcome this drawback.[44,83,84] For example, a recent study showed that a nanogap-based H_2 On–Off sensor using an elastomeric substrate could detect H_2 concentrations as low as 0.01%.[84] Importantly, the elastomeric substrate plays a key role in lowering the detection limit, and the details of this principle and sensing properties are discussed further in section 3.6.

3. Nanogap Design

Numerous studies have been conducted on nanogap-based H_2 sensors, but only a few have focused specifically on design rules for producing nanogaps. The H_2-sensing properties of the nanogap-based H_2 sensors are strongly influenced by nanogap size, fabrication methods, and substrates. As a result, the design of nanogaps is a critical key for realizing an optimized H_2 sensor. This chapter discusses the categorized design rules for making nanogaps and introduces recent developments in the use of elastomeric substrates.

3.1. Fracture Generation by H_2 Exposure

Cracks are not generally induced in thin films and nanowires that are deposited by physical vapor deposition after exposure to H_2. This is due to the fact that the bonding force between substrate and deposited Pd is much stronger than the recovery strength of Pd to equilibrium dimensions. Based on a previous study,[76] sputtered Pd films with a thickness of 100 nm exhibited peel-off traces like large blisters with serious wrinkles when the films underwent α to β phase transition, the result of which is due to stress relief being constrained to local areas of sputtered Pd films by the strong bonding force between the substrate and film. Indeed, unlike physical deposition, Pd structures fabricated by chemical methods exhibit comparatively less bonding strength, such that nanogaps are easily generated on their structures during recovery to their equilibrium dimensions after H_2 exposure (Figure 2).[1,15–19] In addition, cracks are induced in Pd films that are physically deposited on elastomeric substrates simply after undergoing H_2 absorption and desorption.[83] The details of this principle and its sensing properties are discussed further in Section 3.6.

Nanogap formation in Pd was first demonstrated a decade ago (Figure 2b).[1] Mesowires composed of electrodeposited Pd nanoparticles on step edges of single-crystalline graphite were initially electrically conductive. However, after a cycle of H_2 exposure, there was a volume contraction of Pd nanoparticles, and thus nanogaps between Pd nanoparticles were created. As a result, there was no electrical current flow any longer, thereby making the mesowires an On–Off sensor. On the other hand, mesowire structures function as always-On sensors when nanoparticles are positioned too densely for nanogaps to be generated. Although the first demonstration verified that Pd nanogaps could substantially improve H_2-sensing capabilities,

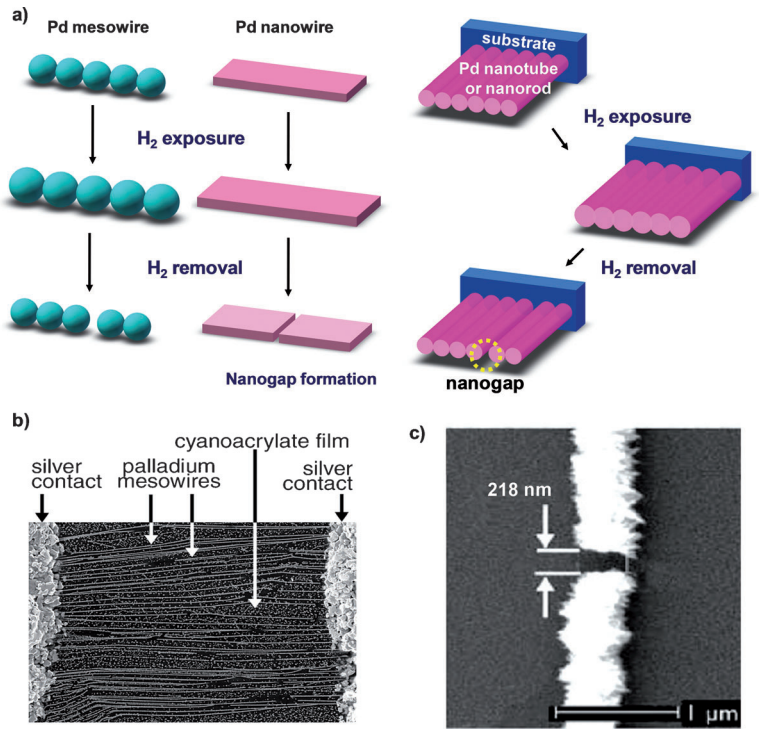

Figure 2. Gap generation by H_2 exposure. a) Schematics of the nanogap generation techniques by H_2 exposure. b) Representative SEM image of a Pd mesowire array. Reproduced with permission from ref. [1]. c) Representative SEM image of a Pd nanowire deposited in the EDTA-containing electrolyte with fractures produced by H_2 exposure. Reproduced with permission from ref. [16].

it also revealed a shortcoming for detecting low concentrations of H_2, namely, a detection limit of 2.25% and 0.5% for On–Off and always-On sensors, respectively.

Other types of nanogap-based sensors have also been studied.[15–19] For instance, sensors based on Pd nanowires have been fabricated by both electrodeposition and electrophoresis methods.[16,17] Nanogaps play a pivotal role in the operation of these sensors. As an interesting example, an array of vertically aligned conoidal Pd nanotubes was shown to form nanogaps through strain accumulation and relaxation during H_2 absorption and desorption processes.[18] The resulting sensors were shown to operate via opening and closing nanogaps upon exposure to H_2.

There are advantages and disadvantages associated with the generation of nanogaps by the H_2 exposure method. The method is simple and provides perfect nanogaps, and thus the resulting sensors exhibit perfect On–Off switching, short response time, and good reversibility. On the other hand, this method does not enable precise control over the gap width, as it depends on the recovery behavior to equilibrium dimensions, which is highly affected by H_2 concentrations and Pd structures. Consequently, the issues associated with decreasing detection limits, which rely on nanogap width, remain an area of active investigation.

3.2. Deposition on Prestructured Patterns

Use of templates is the most widely used approach for nanogap fabrication owing to its ease of use, especially as it requires only physical or chemical deposition of Pd on pre-structured templates. In this method, the final structures and number of nanogaps are dictated by the pre-structured templates. Figure 3a shows a simple schematic for the fabrication of Pd nanogap structures using a prestructured template. Porous structures such as porous Si and anodic aluminum oxide (AAO) membranes can also be readily used as pre-structured templates for nanogap-based H_2 sensors.

In several studies, Pd films were deposited on porous Si prestructures using either immersion plating or electron-beam evaporation.[20,21] In these studies, nanogaps were naturally formed because the porous Si prestructures facilitated localized Pd film growth. Further, electrical resistance of Pd nanogap structures decreased upon exposure to H_2. Such Pd-coated rough Si nanowires are depicted in Figure 3b.[23] The Si nanowires were fabricated by simple electroless etching followed by sputter coating of a thin Pd film. Notably, such vertical type sensors exhibit a low detection limit of 5 ppm H_2 in air, along with a short response time. Since such vertical sensors also operate based upon their ability to be connected or disconnected between nanowires in close proximity, it is possible to detect concentrations of H_2 as low as 1000 to 5 ppm. Figure 3c shows the fracture patterns generated by thermal stress on photo-resist stripes used for introducing nanogaps on Pd nanowires.[22] The fracture patterns were found to change as a function of stripe width.

In addition, the formation of vertical nanogaps between any two suspended Pd-coated electrodes and a single fixed bottom electrode has been demonstrated (Figure 3d).[24] Such sensors have a unique structure, and are easily integrated into larger scale sensor arrays. Even though the nanogap widths of such sensors can be reduced to less than 10 nm, they continue to suffer from a high detection limit (about 1.5%) similar to other nanogap sensors. In such cases, Pd islands can be formed by electrodeposition on prepatterned layers,[45] and gaps with several nanometers in width can be obtained. Despite the existence of such narrow nanogaps, these sensors do not behave in an On–Off manner and may fluctuate as a function of base resistance. Thus, active templates have been

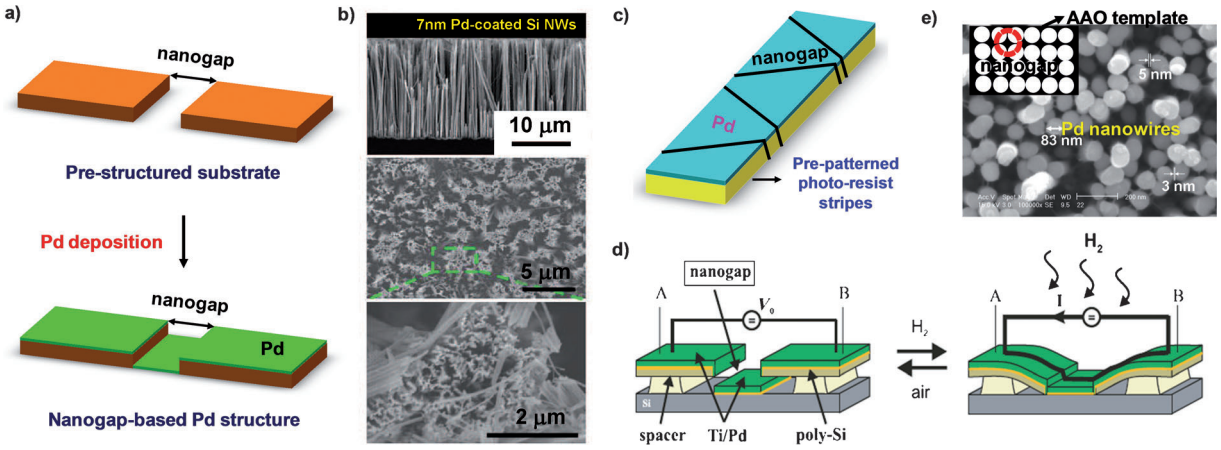

Figure 3. Deposition onto pre-structured patterns. a) Schematic of forming Pd nanogap structures onto pre-structured patterns. b) Representative SEM images of Pd-coated vertical-standing rough Si nanowires. Reproduced with permission from ref. [23]. c) Schematic of nanogap patterns dependent on stripe widths. d) Schematics of the sensing mechanism of suspended Pd/Ti/poly-Si electrodes and a Pd/Ti bottom electrode. Reproduced with permission from ref. [24] e) Representative SEM image of Pd nanowires grown on Si substrate after removing the AAO template. Reproduced with permission from ref. [26].

smartly utilized to introduce nanospacing in electrodeposited Pd nanoarrays.[25] Although the sensing performance of such approaches has not been reported, the basis of this design has been proposed as a new approach for advanced nanogap-based H_2 sensors. Indeed, a H_2 sensor based on electrodeposited Pd nanowires in an anodized aluminum oxide (AAO) template has been shown (Figure 3e), where nanogaps were left behind upon removal of the AAO template.[26]

Use of prestructured templates for the fabrication of nanogaps has increased the options for nanogap design and allows researchers now to seek more possible applications based on nanogaps. Like other types of nanogap-based H_2 sensors, however, sensing performance is highly dependent on how the prepatterns are constructed beforehand. Most sensors in this class exhibit poor H_2-sensing performance. Specifically, not only do they have a high detection limit up to 1.5% H_2 with a long response time when used as On–Off sensors, but they also have disadvantages such as low sensitivity, long response time, and a shift of base resistance when used as always-On sensors.

3.3. Island Formation on a Surface

Nanogaps can also be formed between islands when an extremely thin film is discontinuously deposited on a substrate using a physical deposition method (Figure 4a). The electrical resistance of a discontinuous Pd film decreases by volume expansion of the film upon exposure to H_2 (Figure 4b). However, nanogaps fabricated in this way are unable to allow the nanogap-containing films to operate in an On–Off mode, because the Pd islands form partial conduction paths due to the low island density and large adhesion force between Pd islands and the substrate, which restricts the free lateral motion of Pd. To tackle this issue, there has been an effort to reduce the adhesion force between a discontinuous Pd film and the substrate using a polymer-based buffer layer, thereby easing the lateral expansion of Pd. This is discussed later in this chapter. This method of island formation on a surface is relatively simple and shows decent sensing capabilities such as a short response time and low detection limit.

Figures 4c,d show the nanogap-based sensors fabricated from Pd islands on different substrates and their characteristic response curves. These types of sensors, which are basically fabricated by employing physical deposition methods, have been optimized by some modifications to improve the sensing performance.[28,29] The amount of Pd deposited is a key factor in determining the sensing mechanism. Since the adhesion force between the substrate and a discontinuous film is large enough to restrict the free motion of the Pd film, the sensing characteristics of these sensors usually are determined by mul-

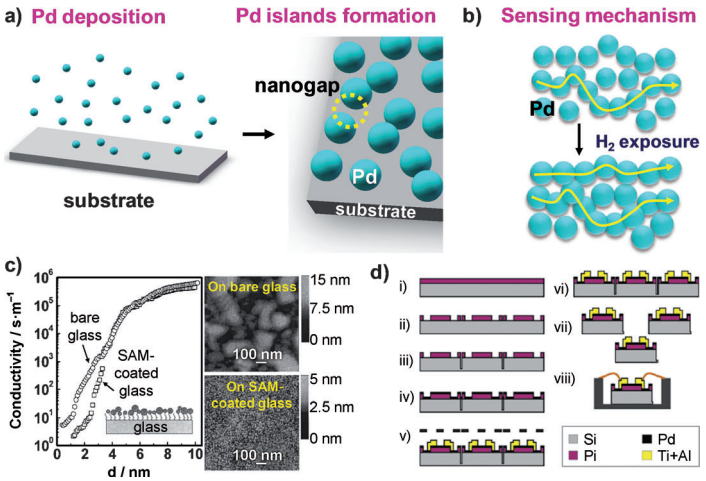

Figure 4. Island formation on a surface. a) Schematic of Pd island formation by physical deposition methods. b) Schematic of the sensing mechanism of the island design. c) Thickness-dependent conductivities of two types of Pd island sensors, respectively, on a siloxane self-assembled monolayer-coated glass and a bare glass. Reproduced with permission from ref. [30]. d) A process flow for sensor fabrication using the deposition of electrodes on a pre-diced substrate. Reproduced with permission from ref. [31].

tiple mechanisms. This means that two mechanisms simultaneously participate in the H_2-sensing process and that a more dominant mechanism is decided by the amount of deposited Pd and the sensing conditions. Specifically, when a small amount of Pd is deposited, a sensor shows a decrease in electrical resistance due to a dominant contribution from the nanogap-closing mechanism. In the other case, where larger amounts of Pd are deposited, both the carrier scattering mechanism and nanogap-closing mechanism can occur, depending on H_2 concentrations at room temperature.[29] For instance, at low concentrations of H_2, the carrier scattering mechanism became dominant while the nanogap-closing mechanism is less influential.

Figure 4c shows a siloxane monolayer coated on a substrate for easing the volume expansion of Pd clusters through reduction in friction between the Pd and substrate.[30] As a result, this sensor showed fast response and a low detection limit of 25 ppm H_2. The key performance enhancement in this case arose from the flexible buffer layer, which helps the movement of Pd clusters. A similar study employed a flexible buffer layer under a discontinuous Pd film deposited by electron-beam evaporation (Figure 4d).[31] Using this technique, the large-scale sensor fabrication and the effects of the flexible buffer layer were demonstrated. As a consequence, the sensors could detect H_2 in the range of 0.5 to 4% with a response time of several seconds and a power consumption of several tens of nW at room temperature.

The simple fabrication process is the most outstanding advantage of the island formation on a surface. Moreover, this method shows great sensing performance such as fast response and low detection limit, compared to other nanogap-based H_2 sensors. However, the sensors fabricated by this method can only operate in always-On mode and may have reproducibility issues because highly delicate control of deposition time is required for fabrication of discontinuous films. Nevertheless, the simple and low-cost sensor fabrication by this method appeals to many researchers studying nanogap-based H_2 sensors, which have suffered from complicated and costly fabrication processes.

3.4. Artificial Manipulation Methods

Nanogaps can also be introduced to Pd structures by an artificial manipulation method, which uses a top-down approach such as focused ion beam milling (FIB). This approach has merit because it is able to achieve precise control over nanogap width. However, in the cases of the other methods described above, their approaches do not offer the levels of engineering control needed for realistic applications.

By employing FIB, the width of a nanogap can be controlled as small as 10 nm (Figure 5a).[34] However, this technique also has its limitations. Typically, some nanogaps are closed after milling, and the widths of nanogaps cannot be reduced below certain sizes, as the thickness of wires decreases. The detection limit is rarely lower than 2.5% H_2, despite the controllable width of nanogaps. Similar to the previous siloxane-inserted Pd islands, sensing performance can be enhanced upon introduction of a polyimide elastic adhesion layer.

The precise size control of nanogaps is a significant merit of this approach. By controlling experimental parameters such as the dose of FIB, it is possible to make nanogaps with a desired width and to reduce the gap width down below 100 nm. However, it is also true that this technique is limited with respect to reducing the width of nanogaps. Specifically, reduction of the nanogap width is restricted due to the gap recovery after ion-beam milling, which is accelerated in wires with a reduced thickness. In some cases, the detection limit reaches 2.5% H_2 and exhibits a slow response. Although this type of sensor appears promising, mostly due to the possibility of nanogap width control, the issue of rather low performance remains to be addressed.

3.5. Methods Using Hybrid Materials

The other novel method for fabricating nanogap-based H_2 sensors is to use hybrid materials on Pd. This approach is simple

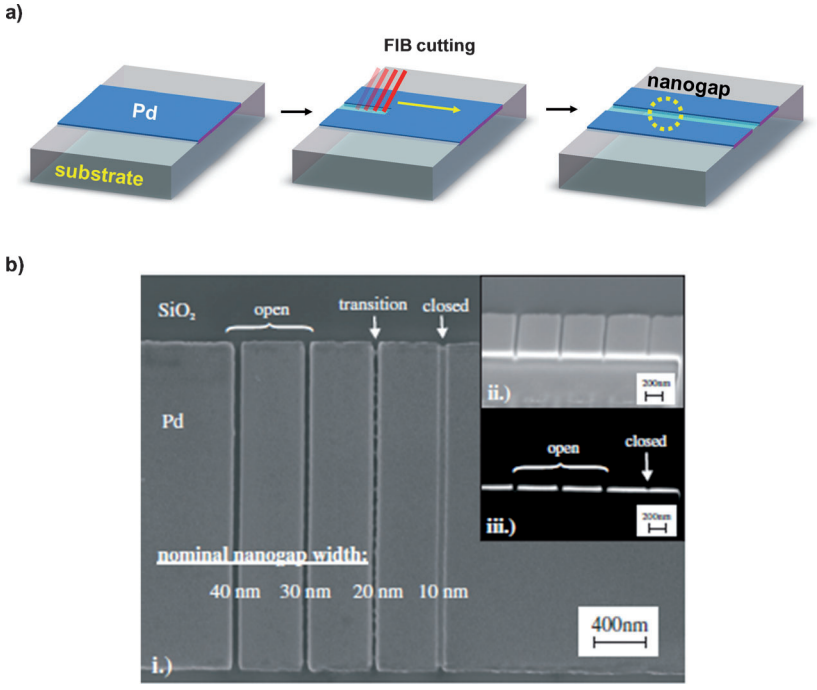

Figure 5. Artificial lithographic methods. a) Schematic of the nanogap fabrication technique using FIB. b) i) SEM image of Pd microwires including nanotrenches with different gap widths of 40, 30, 20, 10 nm, ii) cross-sectional SEM image, and iii) contrast-enhanced SEM image. Reproduced with permission from ref. [34].

in concept: Pd structures are coated with molecules that spatially separate the Pd structures and restrict electrical current flow between neighboring Pd structures or between Pd and electrodes. Upon exposure to H_2, the current flow is enhanced by Pd expansion. This current flow enhancement occurs simply by closing of gaps between Pd structures or between Pd and electrodes. Elaborate processes that coat hybrid materials onto the surface of Pd structures or electrodes are required to realize these sensors.

Figure 6a shows a nanogap fabrication method using hybrid materials coated on Pd nanoparticles.[35–38] The shape and distances between coated materials can be modified by a volume change of the Pd nanoparticles. According to the hybrid structure comprised of hybrid materials, such sensors are able to operate in an "Open–Close" mechanism of nanogaps between Pd nanoparticles, leading to a resistance drop upon H_2 exposure. On the other hand, the lack of structural stability and sensing reliability seemed to be a significant challenge of this approach. As shown in Figure 6b, hybrid materials on the electrodes allow the sensor to detect H_2 by a volume expansion of Pd electrodeposited on the modified electrode.[39,40] This unique structure and the use of hybrid materials allows the sensors to operate in an On–Off manner. In a comparison study, sensors without hybrid materials exhibit a decrease in electrical current when exposed to H_2, indicating that such sensors are governed by the electron-scattering mechanism.

The H_2-sensing properties of these sensors are, however, not effective in terms of sensitivity, response and recovery time, detection limit, and reliability, compared to other types of sensors. This is partly due to the fact that fabrication of the sensors relies on a drop casting method, which makes controlling the amount of Pd nanoparticles difficult. Moreover, since the hybridized structure of Pd and a substrate rarely have a good adhesion at the interface, the motion of Pd often occurs in an unpredicted way during expansion and contraction processes of Pd, resulting in unstable sensing signals in response to H_2. Using the hybrid materials between Pd structures and electrodes, sensors have been shown to behave more reliably. Nevertheless, they still show a weak point in detecting low concentrations of H_2, similar to most other methods. This problem may be alleviated to a certain extent by achieving precise control over hybrid material thickness and also by optimal material selection.

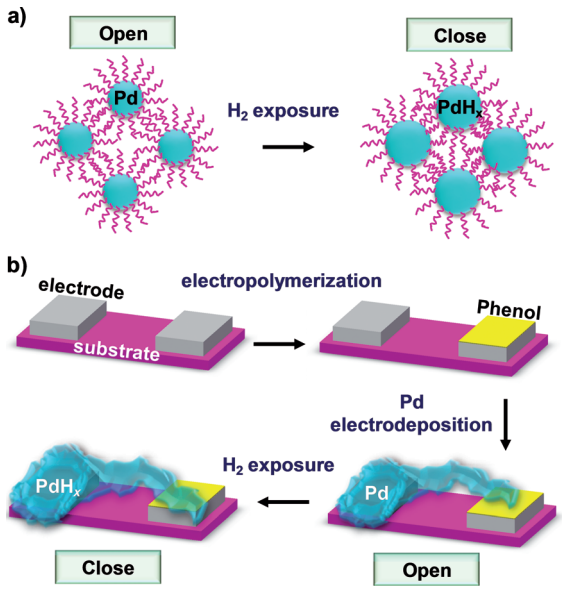

Figure 6. Methods using hybrid materials. a) Schematic of the response of Pd nanoparticles functionalized by hybrid materials to H_2. b) Schematic of the fabrication process for an H_2 switch comprised of hybrid materials.

3.6. Recent Approaches Using an Elastomeric Substrate

Recently, a novel approach to fabricate nanogaps in a Pd-based film using an elastomeric substrate has been reported.[44,83,84] Only stretching the film on an elastomeric substrate was required to generate nanogaps and uniform nanogaps could be created over large areas using this method.[44] This method is called mobile thin film on elastomer (MOTIFE), because the elastomeric substrate act as a mobile support for forming nanogaps and for eliminating the strain at the interface between a thin film and substrate during volumetric changes (Figure 7a). The elastomeric substrate generates roots for propagating nanogaps through a Pd film and help broken Pd films to expand or contract more easily in response to H_2. This is an easy, scalable, and lithography-free nanogap fabrication method.

In a typical experiment, Pd-based MOTIFE sensors are fabricated by a simple stretching route. When the MOTIFE undergoes its first exposure to H_2, H atoms dissolved near the Pd surface and penetrate into the MOTIFE, causing a volume expansion of the Pd film. As a result of this volume expansion, the broken Pd films are brought in contact with each other at both ends. Recovery of the swollen films to their equilibrium dimensions are achieved by desorption of H atoms upon cutting off H_2 flow. This creates nanogaps between the broken Pd films. The Pd-based MOTIFE sensors operate in a perfect On–Off mode with good H_2-sensing characteristics such as the high sensitivity, very fast response and recovery, and good reliability (see Figure 7b). After the first formation of nanogaps, the sensors show reversible sensing cycles between the electrical On and Off states, which correspond to the closed and open states of nanogaps, respectively. Furthermore, the detection limit of these sensors is approximately 0.4% H_2.[44] This value is sufficient to evaluate the potential for commercial products, considering that the most H_2 sensors operating in an On–Off mode can detect H_2 only at a concentration range of 1 to 2% H_2, which is required for the α-to-β phase transition of PdH_x. The detection limit of this class of sensors has been further decreased by adopting PdNi instead of Pd as a sensing material. Indeed, PdNi-based MOTIFE sensors are able to detect H_2 concentrations as low as 800 ppm while maintaining stable On–Off operation.[44] A fabrication process of Pd nanocracks without the application of any external forces has also been demonstrated.[83] Specifically, nanocracks were formed simply by exposure of a Pd thin film to a sufficiently high concentration of H_2 to induce phase transition in the Pd thin film. These sensors possessing nanocracks are formed through

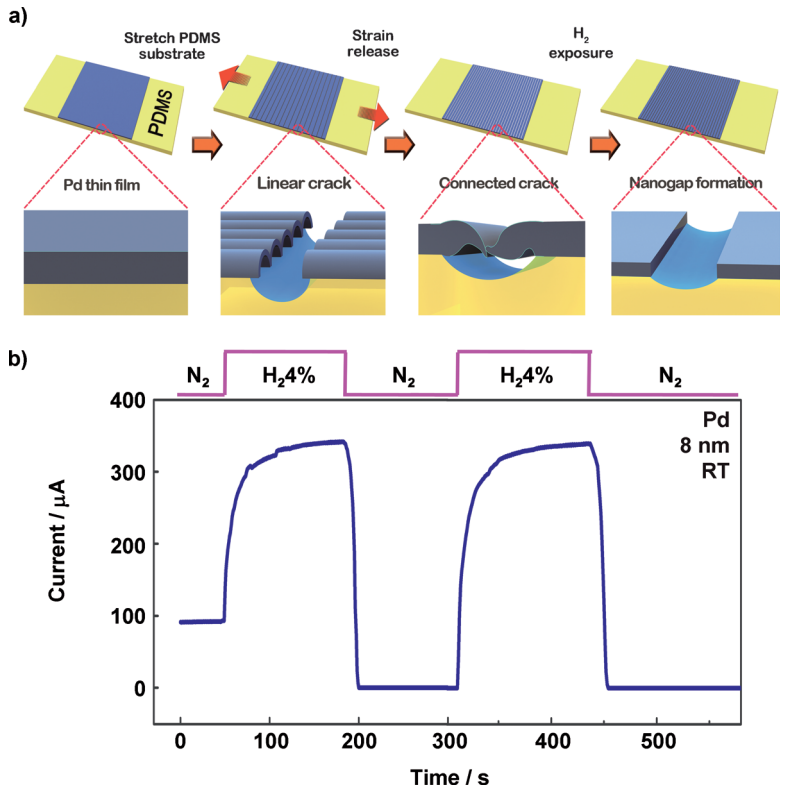

Figure 7. Recent approaches using an elastomeric substrate. a) Schematic of the fabrication process of a Pd-based MOTIFE sensor. b) Representative real-time electrical responses of a Pd-based MOTIFE upon exposure to 4% H_2 at room temperature. Reproduced with permission from ref. [44].

a simple two-step process, namely Pd film deposition followed by exposure to H_2, operated in near-perfect On–Off mode. Such sensors can also detect H_2 concentrations as low as 0.4% and have opened up the possibility for manufacturers to readily produce high-quality nanogap-based H_2 sensors by a simple and low-cost process.

These novel approaches demonstrate the feasibility of manufacturing nanogap-based high-performance H_2 sensors with many advantages. It is true that there have been some efforts to ease Pd expansion and recovery processes. Inserting a polymer-like layer between Pd structures and a substrate and using a flexible substrate like a poly(ethylene terephthalate) (PET) sheet for CNT-based H_2 sensors are typical examples.[60] However, the whole replacement of hard substrates by an elastomeric substrate is the first attempt, to the best of our knowledge. Taking a step forward, it may be even possible to extend this method of fabricating nanogaps to many fields, such as lithography, electronics, photonics, and other interdisciplinary research.

4. Summary

The concept of nanogap-based H_2 sensors has been widely used to meet the requirements of the targeted applications and emerging needs of industries. In general, nanogap-based sensors, operated by an "Open–Close" mechanism, have many advantages such as a fast response, extremely high sensitivity, and reliability over conventional sensors whose mechanisms are based on the electron scattering mechanisms. On the other hand, some disadvantages such as poor detection limit and complex fabrication methods have remained as challenges to be addressed. A variety of approaches have been taken to tackle these issues and help find important platforms that can be utilized for designing nanogap-based sensors with enhanced sensing properties, better reliability, and an easier fabrication process.

Existing nanogap designs and methods have both strengths and weaknesses. For example, nanogaps produced by exposure to H_2 are easy to fabricate, but they are highly dependent on H_2 concentrations and the adhesion force between Pd structures and substrates, resulting in poor control over gap width and a high detection limit. As another example, the film deposition method on prestructured patterns allowed for a control over nanogap width by regulating prestructured patterns. For most approaches categorized in this method, however, the shape of prestructured patterns is hard to control and the sensing properties of the nanogap-containing sensors are thus poor, particularly for always-On type sensors. Reflecting on this method, a simple fabrication process of nanogaps is an essential requisite for their commercialization. In this regard, island formation on a surface is a method that may attract manufacturers due to the simple deposition process. Despite its technical simplicity, the sensors do not always operate in an On–Off manner because the density of Pd clusters on the substrate is too low to close the gaps during Pd volume expansion upon exposure to H_2. Alternatively, efforts have been made to increase the adhesion forces between discontinuous films and substrates by inserting a polymer-based layer, which has shown good sensing performance such as a low detection limit and short response time. In spite of promising results, the reliability of this approach remains a question, since different results have been obtained from similar approaches using the island formation on a surface method.

Controlling the width of nanogaps has long been one of the biggest challenges to many researchers. The reduction of nanogap width is in demand since the optimal sensing properties can be achieved in minimized gaps. Precise nanogap width control can be achieved by using a top-down approach. Indeed, nanogaps as narrow as 30 nm can be formed using this method, and sensors with such nanogaps behave in an

Table 1. Comparison of key features of nanogap-utilizing H_2 sensors.

Fabrication method	Operation type	Detection range [% H_2]	Response time	Cyclability	Manufacturability	Reference
Fracture generation by H_2 exposure	On–Off /On	2.25 ~ 10 /0.5 ~ 10	no mention /70 to 75 ms at 5% H_2	Medium	Difficult	[1] ([1, 15–19])
Deposition onto pre-structured patterns	On	0.2 ~ 1	700 ms at 1% H_2	Medium	Medium	[26] ([20–27])
Island formation on a surface	On	0.25 ~ 5	5 ~ 30 s at 0.25 ~ 5% H_2	Low	Easy	[29] [28–33]
Artificial manipulation methods	On–Off	2.5 ~ 10	9 s at 10% H_2	Low	Medium	[34]
Methods using hybrid materials	On	0.1 ~ 1	3 ~ 5 min at 1% H_2	Low	Difficult	[36] [35–40]
MOTIFE	On–Off	0.4 ~ 10	~0.67 s at 2% H_2	High	Easy	[44] [44, 83, 84]

On–Off manner. However, it is difficult to detect low H_2 concentrations below 2% with such sensors, and extremely narrow nanogaps with a width below 20 nm have not been realized using this technique. Thus, new methods that use hybrid materials on the surface of Pd or an electrode have been proposed. The concept of these approaches is simple, in the sense that pressing a barrier material by the expansion of Pd leads to an increase in electrical conductivity. However, these approaches have remained a challenge because unstable sensing signals make it difficult to detect H_2 concentrations accurately and the performance of sensors fabricated in this way is not reproducible. The use of an elastomeric substrate has been considered as a promising way to fabricate nanogaps. However, this method is still in its early stages, and a study on nanogap width control and quantitative analyses of the degree of recovery to equilibrium dimensions depending on H_2 concentrations should be performed. The key attributes of the respective methods mentioned above are summarized in Table 1.

It is fair to conclude that optimal nanogap-based H_2 sensors cannot be realized without solving the limitations that all the nanogap-based sensors face. For instance, the recently developed nanogap-based H_2 sensors using an elastomeric substrate offer a new paradigm of problem-solving methodology in a sense that they take the advantage of motion-synchronizable substrates rather than modifying sensing materials or structures. As a consequence, the nanogap H_2 sensors that employ an elastomeric substrate can achieve several important features, such as a low detection limit, fast response, easy fabrication, and On–Off operation, leading toward an optimal sensor. However, even these types of H_2 sensors are still away from ideal sensors due to the new constraints, such as thermal instability. Alternative approaches will be likely taken to tackle such new issues. As learned from this example, a single approach is unlikely to solve all the issues and meet the requirements for realizing optimal sensors. Instead, it is highly predicted that combinatorial approaches that merge advantages of multiple technologies will be pursued in designing new nanogap-based H_2 sensors with even more improved performance. Such approaches will allow advanced H_2 sensors, which overcome existing shortcomings, strengthen the respective advantages, and even realize new functions.

Acknowledgements

This work was supported by Priority Research Centers Program through the National Research Foundation of Korea (NRF) funded by the Ministry of Education, Science and Technology (2009-0093823).

Keywords: gap design · gaps · hydrogen gas sensors · palladium · volume expansion

[1] F. Favier, E. C. Walter, M. P. Zach, T. Benter, R. M. Penner, *Science* **2001**, *293*, 2227 – 2231.
[2] D. Porath, A. Bezryadin, S. Vries, C. Dekker, *Nature* **2000**, *403*, 635 – 638.
[3] C. Chen, F. Ko, C. Chen, T. Liu, E. Y. Chang, Y. Yang, S. Yan, T. Chu, *Appl. Phys. Lett.* **2007**, *91*, 253103.
[4] S. Roy, Z. Q. Gao, *Nano Today* **2009**, *4*, 318 – 334.
[5] S. W. Wu, N. Ogawa, W. Ho, *Science* **2006**, *312*, 1362 – 1365.
[6] L. Venkataraman, J. E. Klare, C. Nuckolls, M. S. Hybertsen, M. L. Steigerwald, *Nature* **2006**, *442*, 904 – 907.
[7] A. A. Kornyshev, A. M. Kuznetsov, J. Ulstrup, *Proc. Natl. Acad. Sci. USA* **2006**, *103*, 6799 – 6804.
[8] Z. J. Donhauser, B. A. Mantooth, K. F. Kelly, L. A. Bumm, J. D. Monnell, J. J. Stapleton, D. W. Price Jr., A. M. Rawlett, D. L. Allara, J. M. Tour, P. S. Weiss, *Science* **2001**, *292*, 2303 – 2307.
[9] C. P. Collier, G. Mattersteig, E. W. Wong, Y. Luo, K. Beverly, J. Sampaio, F. M. Raymo, J. F. Stoddart, J. R. Heath, *Science* **2000**, *289*, 1172 – 1175.
[10] A. S. Blum, J. G. Kushmerick, D. P. Long, C. H. Patterson, J. C. Yang, J. C. Henderson, Y. Yao, J. M. Tour, R. Shashidhar, B. R. Ratna, *Nat. mater.* **2005**, *4*, 167 – 172.
[11] W. Jia, L. Su, Y. Ding, A. Schempf, Y. Wang, Y. Lei, *J. Phys. Chem. C* **2009**, *113*, 16402 – 16407.
[12] D. R. Baselt, B. Fruhberger, E. Klaassen, S. Cemalovic, C. L. Britton Jr., S. V. Patel, T. E. Mlsna, D. McCorkle, B. Warmack, *Sens. Actuators B* **2003**, *88*, 120 – 131.
[13] S. Mubeen, B, Yoo, N. V. Myung, *Appl. Phys. Lett.* **2008**, *93*, 133111.
[14] F. J. Ibañez, F. P. Zamborini, *J. Am. Chem. Soc.* **2008**, *130*, 622 – 633.
[15] E. C. Walter, F. Favier, R. M. Penner, *Anal. Chem.* **2002**, *74*, 1546 – 1553.
[16] F. Yang, D. K. Taggart, R. M. Penner, *Nano Lett.* **2009**, *9*, 2177 – 2182.
[17] V. La Ferrara, B. Alfano, E. Massera, G. D. Francia, *IEEE Trans. Nanotech.* **2008**, *7*, 776 – 781.
[18] S. Cherevko, N. Kulyk, J. Fu, C. Chung, *Sens. Actuators B* **2009**, *136*, 388 – 391.
[19] M. Z. Atashbar, S. Singamaneni, *Sens. Actuators B* **2005**, *111 – 112*, 13 – 21.
[20] K. Luongo, A. Sine, S. Bhansali, *Sens. Actuators B* **2005**, *111 – 112*, 125 – 129.
[21] Haohao Lin, Ting Gao, Joshua Fantini, Michael J. Sailor, *Langmuir* **2004**, *20*, 5104 – 5108.

[22] S. Jebril, M. Elbahri, G. Titazu, K. Subannajui, S. Essa, F. Niebelschutz, C. Rohlig, V. Cimalla, O. Ambacher, B. Schmidt, D. Kabiraj, D. Avasti, R. Adelung, *Small* **2008**, *4*, 2214 – 2221.
[23] J. Noh, H. Kim, B. S. Kim, E. Lee, H. H. Cho, W. Lee, *J. Mater. Chem.* **2011**, *21*, 15935 – 15939.
[24] T. Kiefer, A. Salette, L. G. Villanueva, J. Brugger, *J. Micromech. Microeng.* **2010**, *20*, 105019.
[25] D. Bera, S. C. Kuiry, Z. U. Rahman, S. Seal, *J. Electrochem. Soc.* **2005**, *152*, C566-C570.
[26] K. T. Kim, S. J. Sim, S. M. Cho, *IEEE Sens. J.* **2006**, *6*, 509 – 513.
[27] K. T. Kim, S. M. Cho, *IEEE Sens. J.* **2004**, *4*, 705 – 707.
[28] J. van Lith, A. Lassesson, S. A. Brown, M. Schulze, J. G. Partridge, A. Ayesh, *Appl. Phys. Lett.* **2007**, *91*, 181910.
[29] M. Khanuja, S. Kala, B. R. Mehta, F. E. Kruis, *Nanotechnology* **2009**, *20*, 015502.
[30] T. Xu, M. P. Zach, Z. L. Xiao, D. Rosenmann, U. Welp, W. K. Kwok, G. W. Crabtree, *Appl. Phys. Lett.* **2005**, *86*, 203104.
[31] T. Kiefer, L. G. Villanueva, F. Fargier, F. Favier, J. Brugger, *Nanotechnology* **2010**, *21*, 505501.
[32] O. Dankert, A. Pundt, *Appl. Phys. Lett.* **2002**, *81*, 1618 – 1620.
[33] G. Kaltenpoth, P. Schnabel, E. Menke, E. C. Walter, M. Grunze, R. M. Penner, *Anal. Chem.* **2003**, *75*, 4756 – 4765.
[34] T. Kiefer, F. Favier, O. Vazquez-Mena, G. Villanueva, J. Brugger, *Nanotechnology* **2008**, *19*, 125502.
[35] M. Moreno, F. J. Ibanez, J. B. Jasinski, F. P. Zamborini, *J. Am. Chem. Soc.* **2011**, *133*, 4389 – 4397.
[36] Y. Hatakeyama, M. Umetsu, S. Ohara, F. Kawadai, S. Takami, T. Naka, T. Adschiri, *Adv. Mater.* **2008**, *20*, 1122 – 1128.
[37] F. J. Ibañez, F. P. Zamborini, *Langmuir* **2006**, *22*, 9789 – 9796.
[38] S. Ohara, Y. Hatakeyama, M. Umetsu, K. Sato, T. Naka, T. Adschiri, *J. Power Sources* **2009**, *193*, 367 – 370.
[39] R. Dasari, F. P. Zamborini, *J. Am. Chem. Soc.* **2008**, *130*, 16138 – 16139.
[40] R. Dasari, F. J. Ibañez, F. P. Zamborini, *Langmuir* **2011**, *27*, 7285 – 7293.
[41] F. Yang, D. Taggart, R. M. Penner, *Small* **2010**, *6*, 1422 – 1429.
[42] F. Yang, S. Kung, M. Cheng, J. Hemminger, R. M. Penner, *ACS Nano* **2010**, *4*, 5233 – 5244.
[43] A. Gurlo, D. R. Clarke, *Angew. Chem.* **2011**, *123*, 10312 – 10314; *Angew. Chem. Int. Ed.* **2011**, *50*, 10130 – 10132.
[44] J. Lee, W. Shim, E. Lee, J. Noh, W. Lee, *Angew. Chem.* **2011**, *123*, 5413 – 5417; *Angew. Chem. Int. Ed.* **2011**, *50*, 5301 – 5305.
[45] F. Favier, *Procedia Chem.* **2009**, *1*, 746 – 749.
[46] Y. Dan, S. Evoy, A. T. Johnson, *Nanowire Research Progress* **2008**, Chapter 3, 1 – 32.
[47] X. Huang, Y. Choi, *Sens. Actuators B* **2007**, *122*, 659 – 671.
[48] J. Riu, A. Maroto, F. X. Rius, *Talanta* **2006**, *69*, 288 – 301.
[49] A. Pundt, R. Kirchheim, *Annu. Rev. Mater. Res.* **2006**, *36*, 555 – 608.
[50] J. Noh, J. M. Lee, W. Lee, *Sens. J.* **2011**, *11*, 825 – 851.
[51] M. E. Franke, T. J. Koplin, U. Simon, *Small* **2006**, *2*, 36 – 50.
[52] C. Flavin, *Appl. Energy* **1994**, *47*, 123 – 146.
[53] H. Bargthels, W. A. Brocke, K. Bonhoff, P. Julich, *Hydrogen Energy Prog. XI2* **1996**, *2*, 1005 – 1015.
[54] K. Agbossou, R. Chahine, J. Hamelin, F. Laurencelle, A. Anouar, J. M. St-Arnaud, T. K. Bose, *J. Power Sources* **2001**, *96*, 168 – 172.
[55] V. A. Goltsov, T. N. Veziroglu, *Int. J. Hydrogen Energy* **2002**, *27*, 719 – 723.
[56] J. G. Firth, A. Jones, T. A. Jones, *Combust. Flame* **1973**, *20*, 303 – 311.
[57] K. I. Lundström, M. S. Shivaraman, C. M. Svensson, *J. Appl. Phys.* **1975**, *46*, 3876 – 3881.
[58] B. S. Kang, F. Ren, B. P. Gila, C. R. Abernathy, S. J. Pearton, *Appl. Phys. Lett.* **2004**, *84*, 1123 – 1125.
[59] J. Kong, M. G. Chapline, H. Dai, *Adv. Mater.* **2001**, *13*, 1384 – 1386.
[60] Y. Sun, H. H. Wang, *Appl. Phys. Lett.* **2007**, *90*, 213107.
[61] M. H. Yun, N. V. Myung, R. P. Vasquez, C. Lee, E. Menke, R. M. Penner, *Nano Lett.* **2004**, *4*, 419 – 422.
[62] X. Zeng, Y. Wang, H. Deng, M. L. Latimer, Z. Xiao, J. Pearson, T. Xu, H. Wang, U. Welp, G. W. Crabtree, W. Kwok, *ACS Nano* **2011**, *5*, 7443 – 7452.
[63] F. Rumiche, H. H. Wang, W. S. Hu, J. E. Indacochea, M. L. Wang, *Sens. Actuators B* **2008**, *134*, 869 – 877.
[64] P. Pandey, J. K. Srivastava, V. N. Mishra, R. Dwivedi, *Solid State Sci.* **2009**, *11*, 1370 – 1374.
[65] D. Luna-Moreno, D. Monzon-Hernandez, J. Villatoro, G. Badenes, *Sens. Actuators B* **2007**, *125*, 66 – 71.
[66] F. A. Lewis, *The Palladium Hydrogen System*, London, Academic, **1967**.
[67] S. Kishorea, J. A. Nelsonb, J. H. Adairb, P. C. Eklund, *J. Alloys Compd.* **2005**, *389*, 234 – 242.
[68] R. Zacharia, K. Y. Kim, A. K. M. F. Kibria, K. S. Nahm, *Chem. Phys. Lett.* **2005**, *412*, 369 – 375.
[69] M. Yamauchi, R. Ikeda, H. Kitagawa, M. Takata, *J. Phys. Chem. C* **2008**, *112*, 3294 – 3296.
[70] G. Strukul, R. Gavagnin, F. Pinna, E. Modaferri, S. Perathoner, G. Centi, M. Marella, M. Tomaselli, *Catal. Today* **2000**, *55*, 139 – 149.
[71] R. Dittmeyer, V. Höllein, K. Daub, *J. Mol. Catal. A* **2001**, *173*, 135 – 184.
[72] R. C. Hughes, W. K. Schubert, R. J. Buss, *J. Electrochem. Soc.* **1995**, *142*, 249 – 254.
[73] Y. H. Im, C. Lee, R. P. Vasquez, M. A. Bangar, N. V. Myung, E. J. Menke, R. M. Penner, M. H. Yun, *Small* **2006**, *2*, 356 – 358.
[74] K. Baba, U. Miyagawa, K. Watanabe, Y. Sakamoto, T. B. Flanagan, *J. Mater. Sci.* **1990**, *25*, 3910 – 3916.
[75] L. Huang, H. Gong, D. Peng, G. Meng, *Thin Solid Films* **1999**, *345*, 217 – 221.
[76] E. Lee, J. M. Lee, J. H. Koo, W. Lee, T. Lee, *Int. J. Hydrogen Energy* **2010**, *35*, 6984 – 6991.
[77] S. Nakano, S. Yamaura, S. Uchinashi, H. Kimura, A. Inoue, *Sens. Actuators B* **2005**, *104*, 75 – 79.
[78] X. M. H. Huang, M. Manolidis, S. C. Jun, J. Hone, *Appl. Phys. Lett.* **2005**, *86*, 143104.
[79] M. Wang, Y. Feng, *Sens. Actuators B* **2007**, *123*, 101 – 106.
[80] Y. Cheng, Y. Li, D. Lisi, W. M. Wang, *Sens. Actuators B* **1996**, *30*, 11 – 16.
[81] E. Lee, J. M. Lee, J. S. Noh, J. H. Joe, W. Lee, *Thin Solid Films* **2010**, *519*, 880 – 884.
[82] K. R. Kim, J. S. Noh, J. M. Lee, Y. J. Kim, W. Lee, *J. Mater. Sci.* **2011**, *46*, 1597 – 1601.
[83] J. Lee, J. Noh, S. H. Lee, B. Song, H. Jung, W. Kim, W. Lee, *Int. J. Hydrogen Energy* **2012**, *unpublished results*.
[84] E. Lee, J. Lee, J. Noh, S. Maeng, W. Lee, *unpublished results*.

Received: January 9, 2012
Published online on March 23, 2012

